Proceedings of the 9th World Congress on New Technologies (NewTech'23)
Brunel University, London, United Kingdom - August 09-11, 2023
Paper No. ICEPR 138
DOI: 10.11159/icepr23.138

Adsorption Of Organic Dye On Pillared Clays

Hari Desai[1], Kannan A.[1]
[1]Department of Chemical Engineering, Indian Institute of Technology, Madras
Adyar, Chennai, Tamil Nadu, India
haridesai23@gmail.com ; kannan@iitm.ac.in

Abstract **-** Naturally occurring bentonite clay is pillared with Cr-polycations and Al-polycations to overcome the swelling nature of the clay upon contact with water. Chromium Pillared Clay (CrPC) and Aluminium Pillared Clay (AlPC) were characterized using Scanning Electron Microscope, X ray diffraction, Energy dispersive X ray analysis and point of zero charge. The basal spacing increase in the interlamellar space confirmed the successful pillaring of clays. Acid Violet 19 (AV-19) dye was used as model adsorptive. Batch adsorption kinetic studies at ambient conditions revealed that the Pseudo Second Order (PSO) model could characterize the adsorption. The PSO rate constant for CrPC and AlPC were 0.0082 g/mg min and 0.0831 g/mg min, respectively. Langmuir isotherm fitted the equilibrium results for both the adsorption systems. The maximum adsorption capacity for the AV-19 dye on CrPC was 37.54 mg/g, while it was 24.33 mg/g for AlPC at ambient conditions. Thermodynamic analysis showed that the adsorption in both adsorbents was endothermic. The effect of pH on adsorption capacity suggested that electrostatic interactions were the primary contributing mechanism for dye adsorption on CrPC and AlPC. The results showed that the pillared clay adsorbents effectively treated the AV-19 dye-containing wastewater.

Keywords**:** Dyes, Wastewater, Adsorption, Pillared clays, Metal Polycations

1. Introduction

Clay is a well-known adsorbent owing to its porous structure and cation exchange capacity. It is a common, naturally occurring, inexpensive, and environmentally friendly material [1]. Clay minerals are a class of hydrated phyllosilicates. Phyllosilicates are continuous tetrahedral sheets that are linked to octahedral sheets. Natural clay lacks permanent porosity, i.e. it swells upon contact with water [2]. This drawback of clay minerals may be facilely overcome through pillaring. Pillared clays are synthesized by intercalating bulky cations into the clay matrix, which form stable pillars after calcination. Metal polycations such as are the most efficient for developing pillared clays [3].

Dyes are refectory organic compounds widely used in textile and dye manufacturing industries. However, these are significant contributors to the chemical oxygen demand of textile wastewater. This wastewater may be efficiently treated through adsorption. Adsorption is an attractive option as it is versatile in removing organic and inorganic pollutants, especially in very low concentration ranges. Further, it is economical, efficient, easy to operate and maintain, and energy efficient. Pillared clays are efficient adsorbents [4] and have been widely used in both adsorption and catalysis [5], [6], [7]. Studies are scarce on removing Acid Violet 19 (AV-19) dye using pillared clays.

The current study details the application of natural clay pillared with Al polycations (AlPC) and Cr polycations (CrPC) as adsorbents for separating AV-19 from aqueous solutions. The optimal operating conditions, viz. pH and temperature, for the adsorption of AV-19 dye are identified. Finally, a mechanism is proposed for the adsorption of AV-19 dye onto CrPC and AlPC.

2. Materials and Methodology

The CrPC and AlPC were prepared from extra pure bentonite and purchased from Loba Chemie Pvt. Ltd., Mumbai, India. $CrCl_3.6H_2O$ was used as a precursor for the preparation of Cr polycations, $AlCl_3.6H_2O$ was used as a precursor for the preparation of Al polycations, and NaOH was purchased from Loba Chemie Pvt. Ltd., Mumbai, India. CrPC and AlPC were synthesized using the procedure described in [3]. AV-19 was purchased from SRL Pvt. Ltd. Mumbai.

X-ray Diffraction (XRD) spectra were obtained using RIGAKU and SUPERMINI FLEX 6G BENCHTOP (Voltage 40 kV, Current 15 mA) XRD analyzer with CuKβ radiation. The basal spacing was obtained using Bragg's law with a wavelength of 1.387 Å for CuKβ radiation. The surface morphological characteristics were obtained using Hitachi S-4800 Scanning Electron Microscope (SEM). Energy Dispersive X-ray (EDS) analysis used Oxford Instruments (X-MaxN). The

point of zero charge (pHZC), which indicates the nature of a surface charge on the adsorbent surface as a function of pH, was estimated using the method discussed in [3].

Adsorption isotherm experiments were carried out at 300 K, 308 K, and 318 K for 72 h using an orbital shaker (Sub Zero Lab Instruments, Chennai, India) operating at 180 rpm. The volume of dye solutions used was 0.1L. The concentration of dyes before and after adsorption was analyzed using UV–visible spectrophotometer (JASCO UV–Vis V-730). Batch kinetic adsorption experiments were conducted in a 0.5 L stirred vessel at ambient conditions.

Kinetic analysis helps in understanding the rate of dye uptake by the adsorbent. Pseudo first order (PFO) and pseudo second order (PSO) models are commonly used to describe adsorption kinetics that is as described in Eq. (1) and Eq. (2), respectively [3].

$$q_t = q_e\,(1 - e^{-k_1\,t}) \qquad (1)$$

$$q_t = \frac{k_2\,q_e^2\,t}{1+(k_2\,q_e\,t)} \qquad (2)$$

Here k_1 (min^{-1}) and k_2 (g $mg^{-1}min^{-1}$) are pseudo first order and pseudo second order rate constants, t is time (min), and q_t (mg/g) is adsorption capacity at time t.

The Langmuir isotherm is given in Eq. (3). Here, q_e (mg/g) is the equilibrium capacity of the dye adsorbed, Ce (mg/L) is the equilibrium concentration of the dye in the solution, q_{max} (mg/g) is the Langmuir isotherm parameter that estimates the maximum adsorption capacity obtained from the monolayer of the adsorbate formed on the adsorbent surface, and K_L (L/mg) is the Langmuir constant which is related to adsorption energy [8].

$$q_e = \frac{q_{max}K_L C_e}{(1+K_L\,C_e)} \qquad (3)$$

The Freundlich model is given by Eq. (4). Here is the parameter K_F (mg^{1-n}).(L^n /g) is a measure of the adsorbent's capacity. The parameter n (dimensionless) measures adsorption intensity [8]. A lower value of n indicates stronger adsorption.

$$q_e = K_F\,C_e^n \qquad (4)$$

Thermodynamic parameters such as Gibbs free energy (ΔG), enthalpy (ΔH), and entropy (ΔS) for the adsorption of dyes were calculated using Eq. (5)-(7).

$$\Delta G = -R\,T\ln(K_e) \qquad (5)$$

Here T is the absolute temperature (K), R is the universal gas constant, K_e is the dimensionless equilibrium constant as defined by Eq. (6),

$$K_e = \frac{K_L x\ 1000\ x\ \text{Molecular weight of adsorbate}\ x\ [\text{adsorbate}]^o}{\gamma} \qquad (6)$$

Where γ is the activity coefficient (dimensionless) and $[adsorbate]^o$ is the standard concertation of adsorbate (mol/L) [9]. γ was considered unity for dilute solutions [3]. The standard concertation of adsorbate $[adsorbate]^o$ equals 1 mol/L by definition [3].

The relationship between K**e**, ΔH, and ΔS may be described by the van't Hoff correlation as shown by Eq. (7).

$$\ln(K_e) = \frac{\Delta S}{R} - \frac{\Delta H}{R\,T} \qquad (7)$$

The thermodynamic study was made at three different temperature levels: 300, 308, and 318 K. By plotting ln (K**e**) v/s 1/T, ΔH and ΔS were determined from the slope and intercept, respectively.

3. Results and Discussions

3.1 Characterization of Adsorbents

XRD analysis revealed that the basal spacing of bentonite increased post-pillaring from 11.80 Å to 13.20 Å for CrPC and 15 Å for AlPC. This increase in basal spacing post-pillaring showed the successful formation of pillared clays. Hence pillaring with aluminium polycations led to higher basal spacing when compared to that with chromium polycations. Table 1 depicts the elemental composition obtained from EDS. The presence of Cr in CrPC and increased concentration of Al in AlPC shows successful incorporation and pillaring of Cr and Al polycations in CrPC and ALPC, respectively.

Table 1: EDS analysis of Bentonite, CrPC and AlPC on a % basis

Element	O	Na	Mg	Al	Si	Cl	K	Ca	Ti	Fe	Cr
Bentonite	60.75	1.74	1.29	6.53	9.30	0.18	0.20	0.2	10.3	9.51	0
CrPC	51.47	0	1.70	7.7	16.33	0.50	0.44	0	0.50	3.68	17.67
AlPC	55.43	0	1.09	15.54	21.53	0	0.54	0	0.56	5.32	0

Fig. 1 depicts the SEM images of CrPA and AlPC. Particles are present in face-face and face-edge layer aggregations commonly found in Smectite [10]. CrPC and AlPC have fewer face-to-edge and more face-to-face layer formations, possibly due to more ordered morphology in the pillared clays [10]. The raw clay has a tightly packed structure, as seen in [3], but the CrPC and AlPC are more porous, as may be seen in Fig. 1. This change in the morphology of clay may be attributed to a change in the surface charge of particles due to pillaring [6].

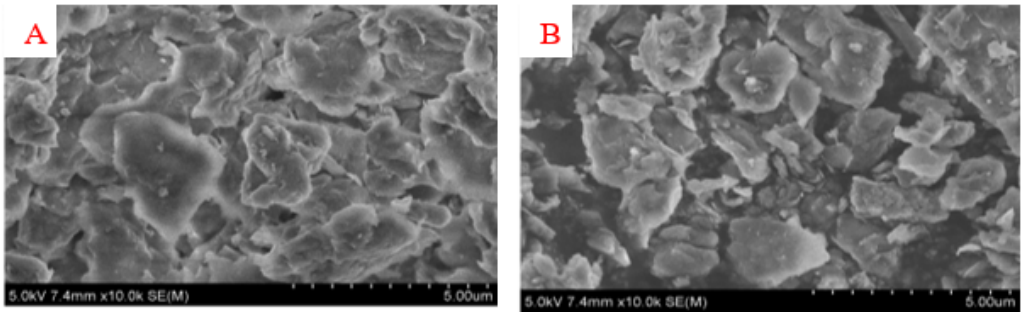

Fig. 1: SEM images of (A) CrPC (B) AlPC

The point of zero charge for bentonite was 8, which dropped to 6 in AlPC and 2.6 in CrPC. When the pH of the solution is below the point of zero charge there arises a net positive charge on the surface. When the pH of the solution exceeds the point of zero charge there is a net negative charge on the adsorbent surface. The reduction in the point of zero charge after pillaring may be attributed to forming of a new acid site in the clay due to the presence of Cr and Al oxides in CrPC and AlPC, respectively.

3.2 Adsorption Kinetic Analysis

Fig. 2 represents the adsorption kinetics of AV-19 dye on CrPC and AlPC. The initial concentration of AV-19 dye was 200 ppm, and the pH was 2 for both CrPC and AlPC. As seen in Fig. 2, the adsorption rate was rapid in the initial 30 minutes but decreased subsequently. Equilibration is attained within 40 minutes for both adsorbents, indicating rapid dye uptake in both cases. The resistance appears more for the convective solute transfer in the aqueous solution rather than internal diffusional rate limitations. The PSO model describes the dye uptake by CrPC and AlPC. Table 2 shows the kinetic parameters for different kinetic models and their corresponding fit statistics. CrPC has a higher equilibrium capacity for AV19 dye than AlPC, even if the latter exhibits a higher adsorption rate. The larger basal spacing in AlPC may have been the reason for faster kinetics.

3.3 Equilibrium adsorption analysis

Fig.3 (A) and (B) represent the adsorption isotherms of AV-19 dye on CrPC and AlPC, respectively. The adsorption equilibria could be well characterized by the Langmuir isotherm for both the adsorbents. The isotherm parameters are summarised in Table 3. This applies to adsorbents with homogeneous surface/active sites [11]. The maximum adsorption capacity of AV-19 dye on CrPC at 300K may be seen at 28.22 mg/g, 1.6 times higher than that of AlPC. As observed from Table 3 and Fig. 3, as the temperature increases, the adsorption capacity increases for both the adsorbents. When the temperature is increased from 300K to 318 K, there is a 76% increase in the adsorption capacity of AV-19 dye on CrPC and

an 81 % increase in AlPC. Similar results were seen in the literature for Acid Blue 74 dye [3],[12] and methyl orange dye [13]. Also, there is an increase in K_L as the temperature increases for both the adsorbent systems.

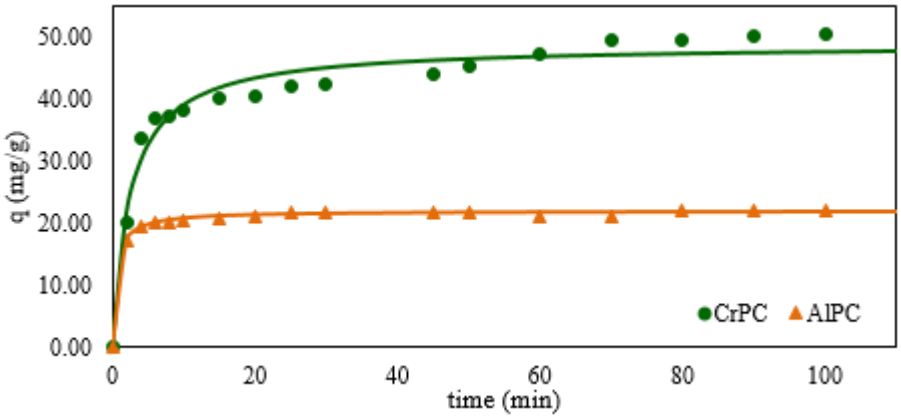

Fig. 2: Adsorption Kinetics of AV-19 on CrPC and AlPC

Table 2: Adsorption kinetic parameters for AV-19 dye on CrPC and AlPC

Pseudo First Order Model	CrPC	AlPC	Pseudo Second Order Model	CrPC	AlPC
k_1 (1/min)	0.27	0.7665	k_2 (g/mg min)	0.0082	0.0831
q_e (mg/g)	45.25	21.24	q_e (mg/g)	48.7	21.83
R^2	0.925	0.989	R^2	0.969	0.995
Adj. R^2	0.92	0.982	Adj. R^2	0.96	0.99

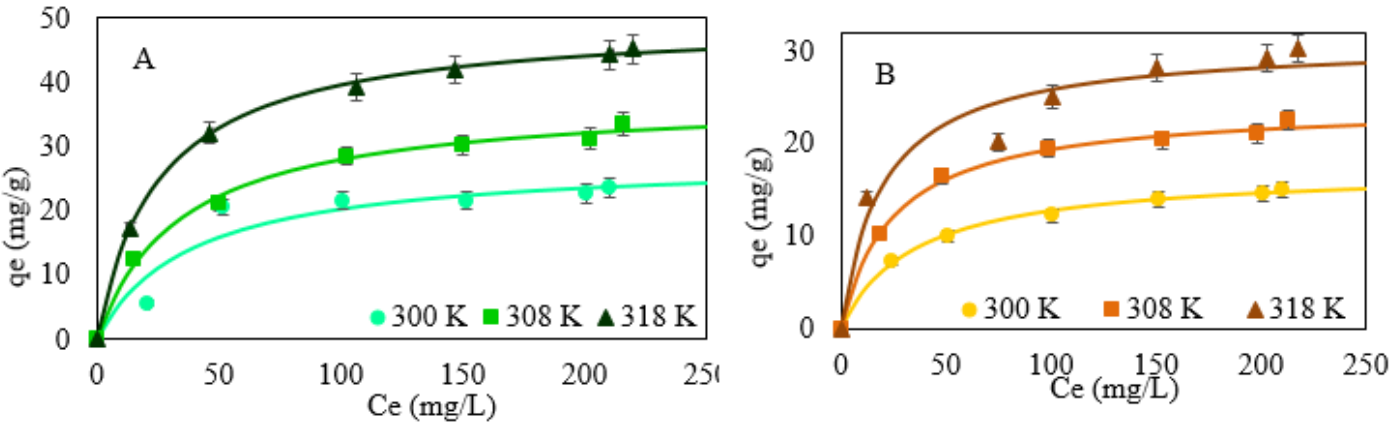

Fig. 3: Isotherm plots at various temperatures for (A) CrPC (B) AlPC

Table 3: Adsorption isotherm parameters for AV-19 dye on CrPC and AlPC at various temperatures

Clays	CrPC			AlPC		
Isotherms	300K	308K	318K	300K	308K	318K
Langmuir Equation						
K_L (L/mg)	0.026	0.029	0.039	0.028	0.039	0.049
q_{max} (mg/g)	28.22	37.54	49.66	17.14	24.33	31.06
R^2	0.925	0.995	0.999	0.997	0.996	0.959
Adj. R^2	0.910	0.993	0.999	0.997	0.995	0.950
Freundlich Equation						
K_F(mg/g)/((mg/L)^n)	4.02	5.65	9.614	2.859	7.495	6.589
n_F	0.338	0.332	0.291	0.311	0.201	0.283
R^2	0.874	0.988	0.986	0.997	0.996	0.991
Adj. R^2	0.849	0.986	0.983	0.996	0.996	0.989

3.4 Thermodynamics analysis of adsorption

Table 4 summarises the thermodynamic parameters for the adsorption of AV-19 dye on CrPC and AlPC. Negative values of ΔG suggest that the adsorption of AV-19 dye on both CrPC and AlPC is spontaneous. The ΔG values for both CrPC and AlPC decrease with temperature increase, indicating the process becomes more spontaneous at higher temperatures. A positive value of ΔH for both CrPC and AlPC suggests endothermic adsorption, as observed by [12], [14]. As seen in Table 4, ΔH values are higher for AlPC than for CrPC, suggesting stronger adsorption on AlPC. The relatively low values of ΔH for CrPC and AlPC (<40 check kJ/mol) imply physisorption [65]. Also, ΔS values for CrPC and AlPC are positive, suggesting increased randomness of the dye molecules on the surface after adsorption. This imples that the adsorption should be carried out at higher temperature for both CrPC and AlPC.

Table 4: Adsorption isotherm parameters for AV-19 dye on CrPC and AlPC at various temperatures.

Dyes	T (K)	ΔG (kJ /mol)	ΔH (kJ /mol)	ΔS (J/K)
CrPC	300	-24.0	17.97	29.37
	308	-24.9		
	318	-26.5		
AlPC	300	-24.2	24.59	52.60
	308	-25.7		
	318	-27.1		

3.5 Effect of pH on adsorption of AV-19 on CrPC and AlPC

Fig.4 depicts the effect of pH on the adsorption of AV-19 dye on CrPC and AlPC. The reduction of q_e with pH may be attributed to the change in adsorbent surface charge with an increase in pH. The adsorbent surface is positively charged below pH 2.6 for CrPC and 6 for AlPC. AV-19 dye is an anionic dye. The–SO_3H groups in the dye have a pKa of -2.6; hence, the dye will have permanent negative centres in the pH range from 2 to 10. At a pH lower than 2.6 for CrPC and 6 for AlPC, there will be an electrostatic attraction between the positively charged surface of CrCP and AlPC and the negatively charged AV-19 dye. The negatively charged –SO_3H groups of the AV-19 dye will be attracted to the Lewis acids sites on CrPC and AlPC introduced by the pillaring process on the clays. At pH higher than 2.6 for CrPC and 6 for AlPC, the AV-19 dye

experiences repulsion between the adsorbents' negatively charged dye and negative surface. The effect of pH on adsorption capacity explains that the interaction between the AV-19 dye and both the adsorbents is driven by electrostatic attraction. This implies that adsorption should be carried out at lower pH for both CrPC and AlPC.

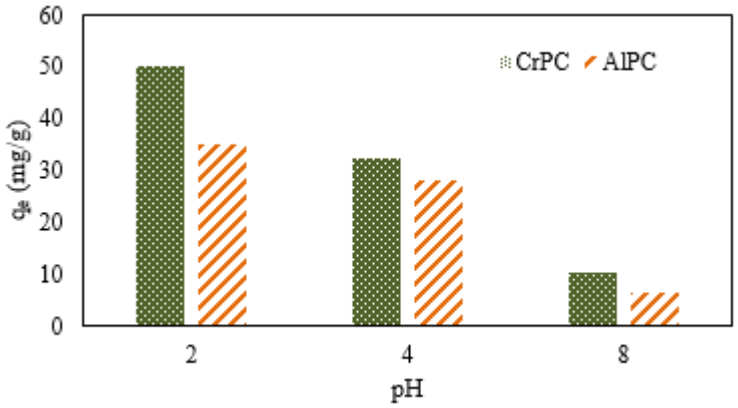

Fig.4: Effect of pH on adsorption of AV-19 dye on CrPC and AlPC

4. Conclusion (T and pH)

Bentonite clay was pillared with Cr and Al polycations. The increase in basal spacing and reduction in the point of zero charge showed that pillaring was successful. These pillared clays were used as adsorbents for the removal of AV-19 dye. Batch adsorption kinetics showed that the system could be represented with PSO kinetic model for both the adsorbents. Langmuir isotherm was a better fit for the representation of the adsorption of AV-19 on both the adsorbents, with CrPC having a higher adsorption capacity than AlPC. Adsorption of AV-19 dye on both CrPC and AlPC was endothermic. The effect of pH on adsorption capacity revealed that electrostatic interactions were the dominant forces to cause the adsorption of AV-19 dye on both AlPC and CrPC. The optimal temperature and pH for maximum adsorption of AV-19 on CrPC and ALPC is 318 K and 2.0 repectively. These results show that CrPC and AlPC are effective adsorbents for textile wastewater treatment.

Acknowledgements

Hari Desai gratefully acknowledges the Department of Science and Technology-INSPIRE Fellowship (IF180532) for financial support. Hari Desai also acknowledges the Indian Institute of Technology, Madras, for providing travel support for this conference (ICEPR-23).

References

[1] Hari, D., Kannan, A., “Synthesis of Pillared Clay Adsorbents and Their Applications in Treatment of Dye Containing Wastewater.,” in *Sustainable Textiles: Production, Processing, Manufacturing & Chemistry. Polymer Technology in Dye-containing Wastewater. In: Khadir, A., Muthu, S.S. (eds)*, 1st ed.Springer, Singapore., 2022, pp. 145–178. [Online]. Available: https://doi.org/10.1007/978-981-19-1516-1_6

[2] F. Bergaya, A. Aouad, and T. Mandalia, “Chapter 7.5 Pillared Clays and Clay Minerals,” in *Developments in Clay Science*, Elsevier, 2006, pp. 393–421. doi: 10.1016/S1572-4352(05)01012-3.

[3] H. Desai, K. A, and G. S. K. Reddy, “Sustainable and rapid pillared clay synthesis with applications in removal of anionic and cationic dyes,” *Microporous Mesoporous Mater.*, vol. 352, p. 112488, Mar. 2023, doi: 10.1016/j.micromeso.2023.112488.

[4] E. Worch, *Adsorption technology in water treatment: fundamentals, processes, and modeling*. Berlin ; Boston: De Gruyter, 2012.
[5] D. L. Guerra, V. P. Lemos, R. S. Angélica, and C. Airoldi, "The modified clay performance in adsorption process of Pb2+ ions from aqueous phase—Thermodynamic study," *Colloids Surf. Physicochem. Eng. Asp.*, vol. 322, no. 1–3, Art. no. 1–3, Jun. 2008, doi: 10.1016/j.colsurfa.2008.02.024.
[6] F. Tomul, "Synthesis, Characterization, and Adsorption Properties of Fe/Cr-Pillared Bentonites," *Ind. Eng. Chem. Res.*, vol. 50, no. 12, pp. 7228–7240, Jun. 2011, doi: 10.1021/ie102073v.
[7] A.-M. Georgescu, F. Nardou, V. Zichil, and I. D. Nistor, "Adsorption of lead(II) ions from aqueous solutions onto Cr-pillared clays," *Appl. Clay Sci.*, vol. 152, pp. 44–50, Feb. 2018, doi: 10.1016/j.clay.2017.10.031.
[8] J. S. Piccin, G. L. Dotto, and L. A. A. Pinto, "Adsorption isotherms and thermochemical data of FD&C Red n° 40 binding by Chitosan," *Braz. J. Chem. Eng.*, vol. 28, no. 2, pp. 295–304, Jun. 2011, doi: 10.1590/S0104-66322011000200014.
[9] M. Hadi Dehghani, R. R. Karri, and E. Lima, *Green technologies for the defluoridation of water*. San Diego: Elsevier, 2021.
[10] Ma. E. Roca Jalil, R. S. Vieira, D. Azevedo, M. Baschini, and K. Sapag, "Improvement in the adsorption of thiabendazole by using aluminum pillared clays," *Appl. Clay Sci.*, vol. 71, pp. 55–63, Jan. 2013, doi: 10.1016/j.clay.2012.11.005.
[11] K. G. Bhattacharyya and S. S. Gupta, "Adsorption of Fe(III), Co(II) and Ni(II) on ZrO–kaolinite and ZrO–montmorillonite surfaces in aqueous medium," *Colloids Surf. Physicochem. Eng. Asp.*, vol. 317, no. 1–3, Art. no. 1–3, Mar. 2008, doi: 10.1016/j.colsurfa.2007.09.037.
[12] A. Muthukkumaran and K. Aravamudan, "Combined Homogeneous Surface Diffusion Model – Design of experiments approach to optimize dye adsorption considering both equilibrium and kinetic aspects," *J. Environ. Manage.*, vol. 204, pp. 424–435, Dec. 2017, doi: 10.1016/j.jenvman.2017.09.010.
[13] B. K. Aziz, D. M. Salh, S. Kaufhold, and P. Bertier, "The High Efficiency of Anionic Dye Removal Using Ce-Al13/Pillared Clay from Darbandikhan Natural Clay," *Molecules*, vol. 24, no. 15, Art. no. 15, Jul. 2019, doi: 10.3390/molecules24152720.
[14] B. K. Aziz, D. M. Salh, S. Kaufhold, and P. Bertier, "The High Efficiency of Anionic Dye Removal Using Ce-Al13/Pillared Clay from Darbandikhan Natural Clay," *Molecules*, vol. 24, no. 15, Art. no. 15, Jul. 2019, doi: 10.3390/molecules24152720.
[15] Y. Cantu *et al.*, "Thermodynamics, kinetics, and activation energy studies of the sorption of chromium(III) and chromium(VI) to a Mn3O4 nanomaterial," *Chem. Eng. J.*, vol. 254, pp. 374–383, Oct. 2014, doi: 10.1016/j.cej.2014.05.110.
[16] E. Worch, *Adsorption technology in water treatment: fundamentals, processes, and modeling*. Berlin ; Boston: De Gruyter, 2012.